Conclusive evidence of quasifission in reactions forming the ^{210}Rn compound nucleus

E. Prasad,[1,*] K. M. Varier,[1] R. G. Thomas,[2] P. Sugathan,[3] A. Jhingan,[3] N. Madhavan,[3] B. R. S. Babu,[1] Rohit Sandal,[4] Sunil Kalkal,[5] S. Appannababu,[6] J. Gehlot,[3] K. S. Golda,[3] S. Nath,[3] A. M. Vinodkumar,[1] B. P. Ajith Kumar,[3] B. V. John,[2] Gayatri Mohanto,[3] M. M. Musthafa,[1] R. Singh,[5] A. K. Sinha,[7] and S. Kailas[2]

[1]*Department of Physics, University of Calicut, Calicut 673635, India*

[2]*Nuclear Physics Division, Bhabha Atomic Research Centre, Mumbai 400085, India*

[3]*Inter University Accelerator Centre, Aruna Asaf Ali Marg, New Delhi 110067, India*

[4]*Department of Physics, Panjab University, Chandigarh 160014, India*

[5]*Department of Physics and Astrophysics, Delhi University, Delhi 110007, India*

[6]*Department of Physics, Faculty of Science, The M.S. University of Baroda, Vadodara 390002, India*

[7]*UGC-DAE CSR, Kolkata Centre, 3/LB-8, Bidhan Nagar, Kolkata 700098, India*

(Received 15 March 2010; published 26 May 2010)

Fission fragment mass ratio distributions have been measured for the reactions ^{16}O + ^{194}Pt and ^{24}Mg + ^{186}W, both leading to the same compound nucleus, ^{210}Rn, at near-barrier energies. The measured fission fragment mass ratio variances for ^{16}O + ^{194}Pt and ^{24}Mg + ^{186}W are compared with the calculations assuming compound nucleus formation. Mass variances of fragments from the ^{24}Mg + ^{186}W reaction show a dramatic deviation from the compound nucleus behavior. This suggests strong evidence for onset of the quasifission process in this reaction.

DOI: 10.1103/PhysRevC.81.054608 PACS number(s): 25.85.Ge, 25.70.Gh, 25.70.Jj

I. INTRODUCTION

The study of fusion-fission dynamics in heavy-ion-induced collisions is a topic of intense research even today. The time evolution of the composite system formed after the reaction and the parameters on which the dynamics depend are still not fully understood. A systematic study of these reactions can reveal information about the complex dynamics involved in the process. Evaporation residues (ERs) are the unambiguous signature of compound nucleus (CN) formation, and considerable efforts are being invested in the study of superheavy elements and superheavy ERs. A major challenge in superheavy element production is the presence of a nonequilibrium process, called quasifission [1–3]. In terms of reaction time scales, quasifission bridges the gap between deep inelastic collisions and CN formation. Deep inelastic reactions represent the energy relaxation mode, exhibiting a wide spectrum of kinetic energy losses [4]. The width of the mass peaks increases with kinetic energy loss, while the centroid of these peaks shows a remarkable stability. On the contrary, CN formation is characterized by full equilibration in all degrees of freedom. Quasifission is a fissionlike process that precedes the formation of a compact mononuclear system and is characterized by total energy relaxation and division of the total mass between the two reaction partners, ranging from initial entrance channel mass asymmetry all the way to symmetry. This process dominates at lower excitation energies, just above the fusion threshold, where ER formation is also maximal, and hence competes strongly with ER formation.

The dynamical models proposed in the early eighties predicted onset of the quasifission process for heavier systems, when the product $Z_P Z_T > 1600$ (where Z_P and Z_T are the atomic charges of the projectile and target, respectively) [1–3]. The observation of anomalous angular anisotropies of fission fragments [5–7] in reactions involving actinide targets over the predictions of transition-state models [8] necessitated the study of the dependence of quasifission on various entrance channel parameters. Entrance channel properties such as mass asymmetry and deformation of the colliding partners are shown to affect the probability of quasifission significantly. It is well known that the entrance channel mass asymmetry $\alpha[\alpha = (A_T - A_P)/(A_T + A_P)]$ (where A_T and A_P are the target and projectile mass, respectively) with respect to the Businaro-Gallone [9] critical mass asymmetry α_{BG} plays a very dominant role in the reaction dynamics [10,11]. For systems with $\alpha > \alpha_{BG}$, the mass flow takes place from the projectile to the target and the composite system leads to the formation of a CN, which may later undergo decay via fission or particle evaporation. On the contrary, if $\alpha < \alpha_{BG}$, the mass flow takes place in the reverse direction, that is, from target to projectile, and a dinuclear system will be formed, which will decay before equilibrating in all degrees of freedom, leading to quasifission. The first experimental signature of nuclear orientation and deformation on quasifission was reported by Hinde *et al.* [12,13] in the ^{16}O + ^{238}U reaction, where the measured fragment angular anisotropies were anomalous over the predictions of statistical models, although the charge product $Z_P Z_T$ was (736 in this case) much less than 1600. To explain the data, an orientation-dependent quasifission process was hypothesized, according to which, if the reaction partners are deformed, at near-barrier energies, tip-to-tip collisions lead to an enhanced probability of quasifission than collisions with flattened sides. Similar experimental results were reported by various groups in reactions involving actinide targets [14,15], supporting the effect of deformation and orientation. The experimental signatures of quasifission include a strong hindrance to ER formation [16,17], anomalous

*prasad.e.nair@gmail.com

fission fragment angular anisotropies [5–7], strong fragment mass angle correlation, and broadened mass distributions [18–21].

In a recent work, Rafie *et al.* [19] measured fission fragment mass distributions in reactions with varying entrance channel mass asymmetry, populating the same composite system ^{202}Po, and concluded the onset of quasifission for the reactions induced by heavier projectiles at near-barrier energies. Thomas *et al.* [20] measured the mass ratio distributions for ^{16}O + ^{204}Pb, ^{34}S + ^{186}W, and ^{48,50}Ti + ^{166,170}Er and reported an increase in the variance of mass ratio distributions at below-barrier energies for ^{34}S and heavier projectiles. Berriman *et al.* [16] measured ER cross sections and fission fragment mass distributions for the CN ^{216}Ra formed through three different entrance channels: ^{12}C + ^{204}Pb, ^{19}F + ^{197}Au, and ^{30}Si + ^{186}W. It was observed that in the case of ^{19}F + ^{197}Au and ^{30}Si + ^{186}W, fragment mass distributions were broader than that for the ^{12}C + ^{204}Pb reaction. A substantial reduction in ER cross sections for ^{19}F- and ^{30}Si-induced reactions was also observed. This reduction in ER cross sections and broadened mass distributions were attributed to the presence of quasifission process in ^{19}F + ^{197}Au and ^{30}Si + ^{186}W systems. However, a series of measurements by Tripathi *et al.* on fission fragment angular distributions for ^{19}F + ^{197}Au [22], ^{24}Mg + ^{192}Os [23], ^{16}O + ^{188}Os, and ^{28}Si + ^{176}Yb [24] at near-barrier energies concluded that the contribution from quasifission is not significant, as the experimental data were successfully explained by statistical model calculations. Appannababu *et al.* [25] have measured fission fragment angular distributions for two systems, ^{11}B + ^{204}Pb and ^{16}O + ^{197}Au, forming the composite system ^{215}Fr and concluded the absence of any non-CN process in these reactions. These measurements leave a question mark on our understanding of the time scales involved in the relaxation of mass and K degrees of freedom. Thus, it becomes imperative to understand the relaxation mechanism of various degrees of freedom, in detail, in less fissile systems.

In the present work, mass angle and mass ratio distribution measurements of the fission fragments in fission of the ^{210}Rn ($\alpha_{BG} = 0.857$) compound system, populated using the ^{16}O + ^{194}Pt ($\alpha = 0.847$) and ^{24}Mg + ^{186}W ($\alpha = 0.771$), reactions have been carried out. The entrance channel mass asymmety of the ^{24}Mg + ^{186}W reaction is much below α_{BG}, while that of ^{16}O + ^{194}Pt is very near α_{BG}. As the targets are deformed (^{194}Pt is oblate deformed and ^{186}W is prolate deformed), the effect of static deformation should also be seen in the reaction dynamics. Measurements have been carried out for both reactions at energies above and below the Coulomb barrier. The excitation energies for both systems match at four different laboratory energies.

II. EXPERIMENT AND ANALYSIS

The experiments were performed at the 15UD Pelletron accelerator facility at the Inter University Accelerator Centre, New Delhi. Two reactions were studied in two separate runs. A pulsed beam of ^{16}O and a dc beam of ^{24}Mg were used in the experiments to bombard an isotopically enriched ^{194}Pt (96.5% enriched) target of thickness 300 μg/cm^2 on carbon foil 20 μg/cm^2 thick and a ^{186}W target (99.5% enriched) of thickness 110 μg/cm^2 on 20 μg/cm^2 carbon backing, respectively. The former reaction is discussed first.

A pulsed beam of ^{16}O with a pulse separation of 250 ns and pulse width of ~1 ns, in the energy range 75 to 102 MeV, was used in the experiment. Two large-area, position-sensitive, multiwire proportional counters (MWPCs) [26] of active area 24 cm × 10 cm were used for fission fragment measurement, by forming a time-of-flight (TOF) setup. These detectors were mounted on the two arms of the scattering chamber: the forward detector centered at polar angle $\theta = 45^\circ$ (azimuthal angle $\phi = 90^\circ$) and the backward detector centered at $\theta = 115^\circ$ (azimuthal angle $\phi = 270^\circ$). The nearest distance to the forward detector from the target was 56 cm and that to the backward detector was 30 cm. The target was kept at 45° with respect to beam direction, which minimized the energy loss of the fragments and also avoided the shadowing of the detectors by the target ladder. The gas detectors were operated with isobutane gas at a low pressure (~3.5 T). The MWPCs provide very good timing and position resolution. The fission fragments were well separated from the elastic and quasielastic channels, in both time and energy loss spectra. Two solid-state detectors, mounted at ±10° with respect to the beam axis, were used to monitor and position the beam at the center of the target throughout the experiment. One of these monitors was used to get the time structure of the beam by generating a TAC signal with an rf signal. The position information of the fragments entering the detectors was obtained from the delay-line readout of the wire planes. The fast timing signal from the anode of both MWPC1 and MWPC2 were used to obtain the TOF of the fragments with respect to the beam pulse. These anode signals were processed by constant fraction discriminators. A fast coincidence between any of the anode signals and the rf pulse was used as the master trigger for the data acquisition system.

In the case of the ^{24}Mg + ^{186}W system, the detectors used were slightly smaller with an active area of 20 cm × 10 cm [27]. The forward detector was centered at polar angle $\theta = 38^\circ$ (azimuthal angle $\phi = 90^\circ$) and the backward detector was centered at $\theta = 113^\circ$ (azimuthal angle $\phi = 270^\circ$). The nearest distance to the forward detector from the target was 55.5 cm, and that to the backward detector was 40 cm. As the beam current was very low for ^{24}Mg in the required energy range, a dc beam was used in the measurements (in the energy range 111 to 125 MeV in the laboratory frame) and the time difference method was used for obtaining the mass ratio distributions of the complimentary fragments. In the case of the ^{16}O + ^{194}Pt reaction, we used the TOF method for getting the mass ratio distributions for some energies and it was verified that both TOF and time difference methods gave the same results. Hence, the latter method was adopted for the analysis, for consistency. It is worth mentioning that the basic assumption in the time difference method is the presence of only full momentum-transfer fission events, and it cannot be adopted for reactions where incomplete momentum-transfer events such as transfer-induced fission are present. But in the present measurements, as the targets used are not fissile, the probabilty of transfer-induced fission is absent. Any of

the signals of the two MWPCs and two monitor detectors formed the master strobe for the data acquisition system in this measurement. Individual TDCs were used for individual MWPCs, with the anode as the start and four position signals as individual stops. A TAC signal was formed by taking the start from the anode signal from the back detector and the stop from the delayed anode signal from the front detector.

The position calibrations of the detectors were performed using the known positions of the edges of the illuminated areas of the detectors during the experiment and, later, by using a fission source (^{252}Cf) of known strength. A mask with holes of 1-mm diameter, separated by 5 mm in the XY plane, was placed in between the source and the detector and fragments were collected. The position resolution of the detectors was better than 1.5 mm. The calibrated positions (X and Y) were converted to polar angles θ and ϕ, and fragment velocities in the laboratory frame were calculated using TOF, θ, and ϕ information. The center-of-mass velocities $v_{1\text{c.m.}}$ and $v_{2\text{c.m.}}$ of the fragments m_1 and m_2, respectively, were then obtained from laboratory velocities using kinematic transformations. The mass distributions and mass ratio distributions of the fragments were obtained event by event using the procedure described in Ref. [28]. The delay δt_0 in Ref. [28] was corrected for each energy during the analysis of the $^{16}\text{O} + ^{194}\text{Pt}$ run assuming symmetric mass division and Viola systematics [29]. In the second run ($^{24}\text{Mg} + ^{186}\text{W}$), the $^{16}\text{O} + ^{197}\text{Au}$ reaction, which is expected to undergo fission through pure CN formation, was used as the calibration system for measuring the electronic time delay involved in the measurements. In this calibration run, both gas detectors were kept at 90° in the center-of-mass frame and the fragments were collected at 90-MeV beam energy. The electronic time delay is then obtained through an iterative method, by imposing the condition that mass ratio distribution is reflection symmetric at about 0.5 at $\theta_{\text{c.m.}} = 90°$.

From the conservation of linear momentum,

$$m_1 v_{1\text{c.m.}} = m_2 v_{2\text{c.m.}}, \tag{1}$$

the mass ratio is given by

$$M_R = \frac{m_2}{m_1 + m_2}. \tag{2}$$

III. RESULTS AND DISCUSSION

The mass angle correlation and the mass ratio distributions of the fragments were obtained for both reactions at energies above and below the Coulomb barrier. The mass ratio plotted against the center-of-mass angle of the fragments from the reaction $^{16}\text{O} + ^{194}\text{Pt}$ at $\text{E}_{\text{c.m.}}$ values of 94.0 MeV (well above the Coulomb barrier, $V_B = 76.3$ MeV) and 74.6 MeV (below V_B) are shown in Figs. 1(a) and 1(b), respectively. Figures 1(c) and 1(d) are similar plots for the $^{24}\text{Mg} + ^{186}\text{W}$ reaction, for $E_{\text{c.m.}} = 110.6$ and 100.0 MeV, respectively. No evidence of mass angle correlation was observed for either of the systems, within the angular and energy ranges studied. Because the finite geometry of our detection system limits the most forward and most backward events, a software cut [120° to 130° for the $^{16}\text{O} + ^{194}\text{Pt}$ reaction in Figs. 1(a) and 1(b) and 125° to 135° for the $^{24}\text{Mg} + ^{186}\text{W}$ reaction; Figs. 1(c) and 1(d)]

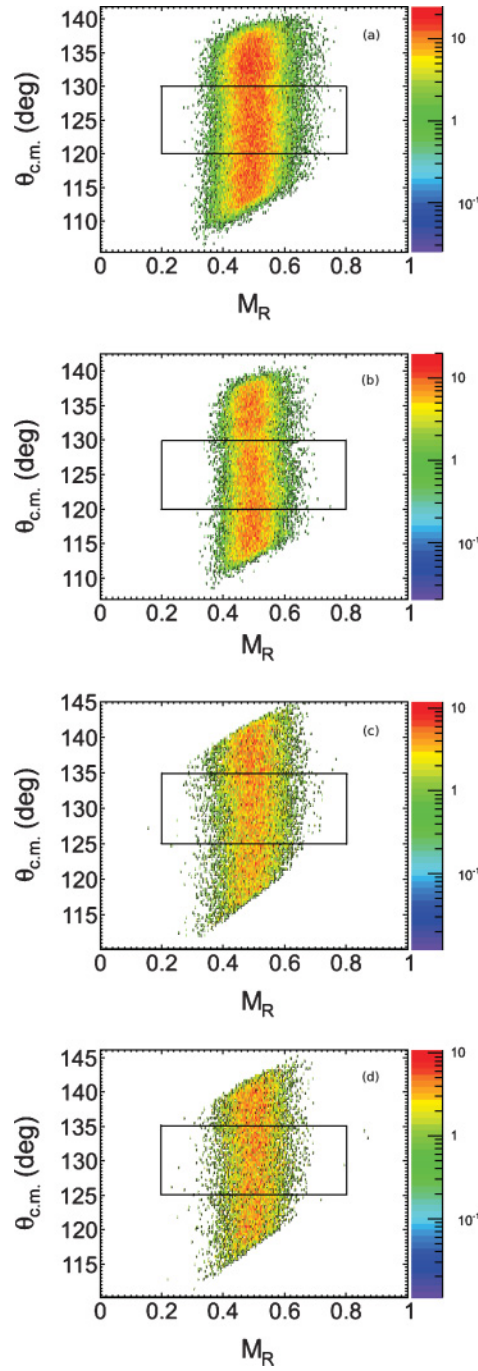

FIG. 1. (Color online) (a, b) Mass ratio versus center-of-mass angle plots for the reaction $^{16}\text{O} + ^{194}\text{Pt}$ at $E_{\text{c.m.}} = 96.0$ and 74.6 MeV, respectively. (c, d) Similar plots for the reaction $^{24}\text{Mg} + ^{186}\text{W}$ at $E_{\text{c.m.}} = 110.6$ and 100.0 MeV, respectively.

was made in the mass density plots as shown in the figures, and only those events that fell inside the window were taken for obtaining the mass ratio distributions. This is very important to avoid any bias of the data coming from the geometrical limitations of the experimental setup. The experimental mass ratio distributions for the $^{16}\text{O} + ^{194}\text{Pt}$ and $^{24}\text{Mg} + ^{186}\text{W}$ reactions at different beam energies are shown in Figs. 2 and 3, respectively. Because shell effects are

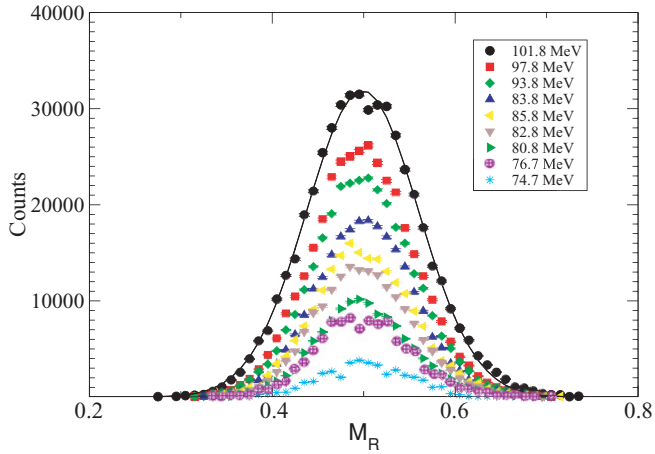

FIG. 2. (Color online) Fission fragment mass ratio distributions at different beam energies for the $^{16}O + ^{194}Pt$ reaction. The distribution is symmetric and centered around $M_R = 0.5$. The solid line is the Gaussian fit to the experimental mass ratio distribution at 101.8-MeV beam energy.

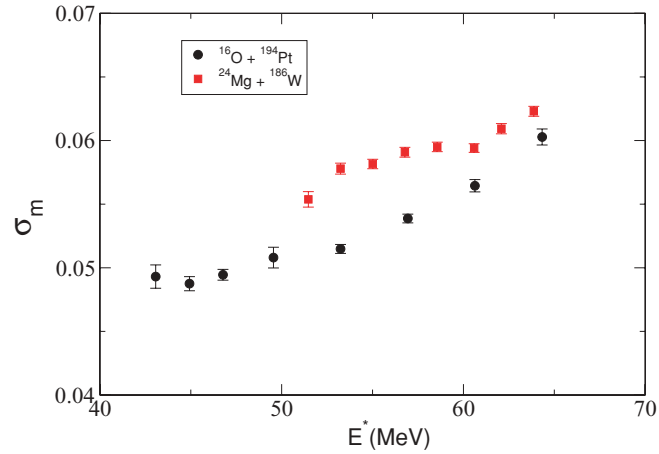

FIG. 4. (Color online) Fragment mass ratio width (σ_m) versus compound nucleus excitation energy for two different entrance channels populating the composite system ^{210}Rn. The mass width is found to increase linearly with the excitation energy in both reactions.

expected to be washed out at higher excitation energies, fragment mass ratio distributions should be symmetric, with the fissionlike fragments centered at $M_R = 0.5$. The width of this distribution increases smoothly with temperature for an equilibrated CN, and a sudden change could be a signature of departure from equilibration. The experimental mass ratio distributions can be easily represented by a Gaussian function with the standard deviation (σ_m) representing the width of the mass ratio distribution. The mass ratio widths (σ_m) plotted against the CN excitation energy are shown in Fig. 4. It shows that σ_m increases with an increase in excitation energy for both reactions. However, at the same excitation energies, the magnitude of σ_m for the $^{24}Mg + ^{186}W$ reaction is higher than that for the $^{16}O + ^{194}Pt$ reaction, and this difference is more pronounced at lower excitation energies (corresponding to near barrier energies). In the energy range studied in the present measurements, the contribution from the fast fission

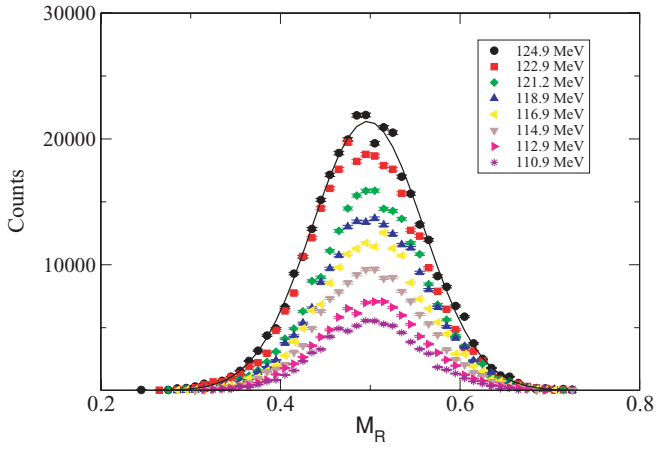

FIG. 3. (Color online) Fission fragment mass ratio distributions at different beam energies for the $^{24}Mg + ^{186}W$ reaction. The solid line is the Gaussian fit to the experimental mass ratio distribution at 124.9-MeV beam energy.

reaction is negligible, as the angular momentum (l) values populated in both reactions are much lower than the critical angular momentum, at which the liquid drop fission barrier B_f [30] vanishes. Pre-equilibrium fission, which is characterized by nonequilibration of K degrees of freedom and hence an enhanced fragment angular anisotropy [31], does not change the mass distribution of the fragments, as mass equilibration is expected to take place before K equilibration and the system would pass over the unconditional fission barrier. The fragment mass distribution, thus, may be a mixture of two possible reaction mechanisms, CN fission and the quasifission reaction. In the case of an equilibrated CN, the variance of the fragment mass distribution is linearly related to the nuclear temperature (T) and the mean square angular momentum $\langle l^2 \rangle$ [32–35]. Hence, it is very important to confirm whether this angular momentum dependence is responsible for the difference in σ_m for the two systems studied. To verify this, variation of $\langle l^2 \rangle$ of the composite system is plotted as a function of excitation energy E^* in Fig. 5. The $\langle l^2 \rangle$ values are calculated using the coupled channels code CCFULL [36], including the rotational couplings (β_2) of the target nucleus. The barrier parameters of the coupled channels code were fixed by reproducing the capture excitation function for the $^{16}O + ^{197}Au$ reaction [37,38], and these values were scaled to get the parameters for the reactions $^{16}O + ^{194}Pt$ and $^{24}Mg + ^{186}W$. From Fig. 5, it is clear that at similar excitation energies, the $\langle l^2 \rangle$ value for the reaction $^{24}Mg + ^{186}W$ is lower than that for the $^{16}O + ^{194}Pt$ reaction, which would not explain the increased mass ratio width for the former reaction. As mentioned before, the mass variance (σ_m^2) of the fragments from an equilibrated composite system is linearly proportional to T and $\langle l^2 \rangle$ [39]:

$$\sigma_m^2 = \lambda T + \kappa \langle l^2 \rangle, \tag{3}$$

where λ and κ are constants. Because the CN undergoes decay via fission as well as particle evaporation, fission $\langle l^2 \rangle$ values used in the calculations were calculated at energies above the Coulomb barrier, using CCFULL and the statistical model code PACE3 [40]. The fusion l distribution obtained from CCFULL

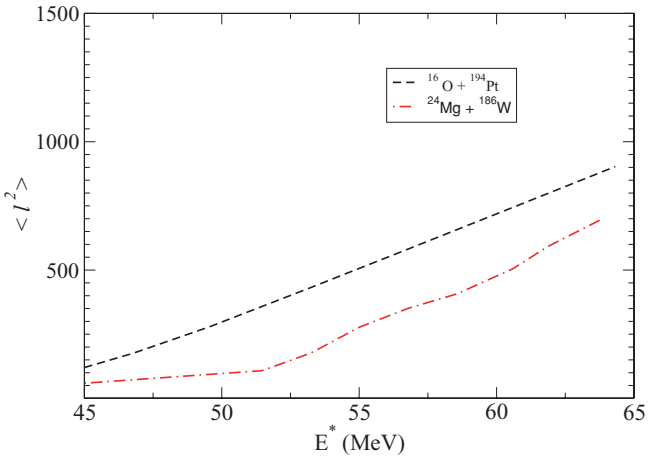

FIG. 5. (Color online) Variation of $\langle l^2 \rangle$ with compound nucleus excitation energy for ^{210}Rn populated by the two entrance channels.

was used as the input to PACE3 in trace back mode and fission $\langle l^2 \rangle$ values were calculated. To further avoid any discrepancy in $\langle l^2 \rangle$ values, the calculations were restricted to higher excitation energies (above 50-MeV excitation, where the fission cross section is dominant over the ER cross section), as lower l values may lead to the formation of ERs. The estimation of nuclear temperature essentially depends on the assumption, whether the properties of the fragments are determined at the saddle point or the scission point. Although in light compound systems, the saddle point and scission point are close to each other, this is not so for heavier systems. However, the estimates of Knyazheva *et al.* [39] in the mass ∼200 region have shown that saddle-point and scission-point temperatures are very similar, and in our calculations we have used the saddle point as the reference point. The saddle-point temperature T is given by

$$T = \sqrt{\frac{E_{\text{c.m.}} + Q - B_f - E_{\text{rot}} - E_{\text{pre}}}{\mathbf{a}}}, \qquad (4)$$

where Q is the "Q" value of the reaction, B_f (fission barrier at average angular momentum) and E_{rot} (average rotational energy at equilibrium deformation) are calculated using the Sierk model [30], E_{pre} is the energy taken away by the neutrons, calculated from the compilation of Saxena *et al.* [41], and **a** ($=A_{\text{CN}}/10$ MeV^{-1}) is the level density parameter.

Because we could not observe any mass angle correlation in the $^{16}O + ^{194}Pt$ reaction and the mass ratio width increases smoothly with E^*, we assumed that this reaction proceeds through the formation of a true CN and the fitting constants λ and κ are determined for this reaction to reproduce the experimental mass ratio variance. If there is no quasifission component in the $^{24}Mg + ^{186}W$ reaction, the obtained constants should reproduce the experimental mass ratio widths for this reaction also. Figure 6(a) shows the experimental and calculated σ_m versus the CN excitation energy for the compound system ^{210}Rn at an excitation energy above 50 MeV. It is shown that calculated values ($\lambda = 2.6 \times 10^{-3} \pm 0.3 \times 10^{-3}$ and $\kappa = 4.9 \times 10^{-7} \pm 0.8 \times 10^{-7}$) do not reproduce the experimentally observed mass width for the $^{24}Mg + ^{186}W$ reaction. This dramatically different

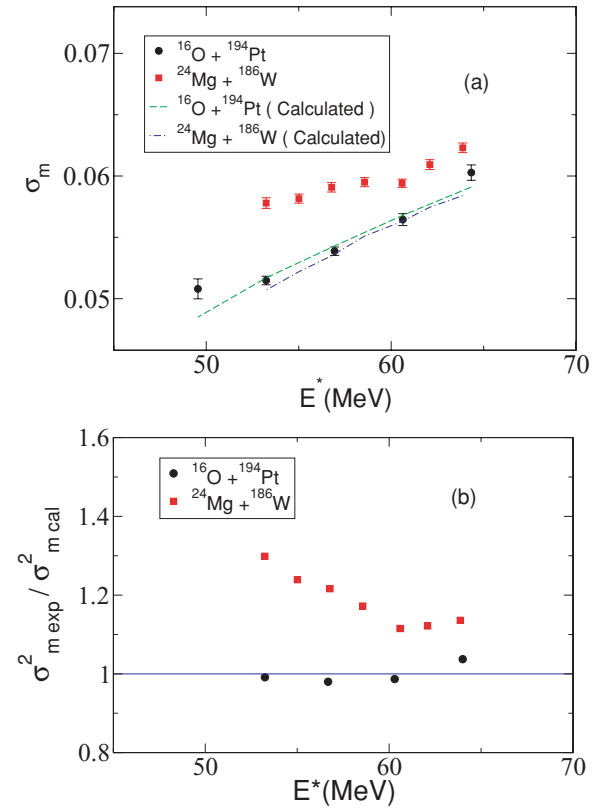

FIG. 6. (Color online) (a) Experimental mass ratio width (σ_m) values for the two reactions compared with the calculations using the fitting constants obtained by assuming compound nucleus fission for the $^{16}O + ^{194}Pt$ reaction. Calculations were performed above 50-MeV excitation. (b) Ratio between the experimental and calculated fragment mass variances $\sigma^2_{m\,\text{exp}}/\sigma^2_{m\,\text{cal}}$ and the compound nucleus excitation energy for the two different entrance channels. A deviation from compound nucleus behavior is observed for the $^{24}Mg + ^{186}W$ reaction, which is a strong signature of onset of the quasifission process in this reaction.

behavior of the mass ratio width could be a strong signature of the deviation of the reaction mechanism from the equilibrated CN process in the $^{24}Mg + ^{186}W$ reaction. In the case of an equilibrated CN, the ratio between the experimental ($\sigma^2_{m\,\text{exp}}$) and the calculated ($\sigma^2_{m\,\text{cal}}$) mass ratio variance is expected to be equal to unity. This ratio plotted against the CN excitation energy for both reactions is displayed in Fig. 6(b). The line at $\sigma^2_{m\,\text{exp}}/\sigma^2_{m\,\text{cal}} = 1$ represents the expected results for the CN assumption. It can be clearly seen that for the reaction $^{16}O + ^{194}Pt$, the values of $\sigma^2_{m\,\text{exp}}/\sigma^2_{m\,\text{cal}}$ are scattered around this line, while the reaction $^{24}Mg + ^{186}W$ shows a remarkable deviation from the line. This deviation, more significant at lower excitation energies (corresponding to near and below the Coulomb barrier), is an obvious signature of the onset of the quasifission process in this reaction.

It is now well known that if two colliding nuclei are heavy, merely overcoming the Coulomb barrier is not a sufficient condition to ensure the formation of a CN, as the electric repulsion dominates over the attractive nuclear force during the dynamical evolution after contact. Hence the effective barrier to overcome for the formation of a CN is not the Coulomb

TABLE I. Parameters (described in the text) of three systems using the same target.

Reaction	χ	χ_e	χ_m	α	α_{BG}	β_2 (projectile)	β_2 (target)
$^{24}Mg + ^{186}W$	0.7350	0.5239	0.6646	0.771	0.851	0.605	0.2257
$^{30}Si + ^{186}W$	0.7504	0.5547	0.6851	0.722	0.865	−0.315	0.2257
$^{34}S + ^{186}W$	0.7688	0.5977	0.7117	0.691	0.874	0.252	0.2257

barrier, but the saddle point in a multidimensional potential energy surface, the same saddle-point that determines the potential energy barrier that protects the CN against fission decay. Hence some extra energy (extra-extra-push [1,3]) is required to induce fusion in a CN, which depends on the mean fissility χ_m of the composite system. The mean fissility χ_m, is a mixture of the CN fissility χ and the effective fissility χ_e, a characteristic of the initial binary system. It is known that quasifission is strongly dependent on χ_m and the extra-extra-push energy calculated [3] shows a dramatic increase around $\chi_m = 0.723$, which was attributed to onset of the quasifission process. Although the properties of the entrance channel are partly incorporated in mean fissility χ_m through effective fissility, χ_e, the effect of deformation, is not included. In this paper, we compare our results with two other systems, $^{30}Si + ^{186}W$ [16] and $^{34}S + ^{186}W$ [20]: both are reported to show deviation from CN behavior. In Table I, we have listed the calculated values of CN fissility χ, effective fissility χ_e, mean fissility χ_m, and static quadrupole deformation (β_2) of projectiles and targets [42]. Although it is quite clear from the calculations that χ_m values for all three reactions, $^{24}Mg + ^{186}W$, $^{30}Si + ^{186}W$, and $^{34}S + ^{186}W$, are less than 0.723, all the reactions show clear evidence of the quasifission process. This suggests that Coulomb repulsion ($Z_P Z_T$), mass asymmetry, static deformation of the reactions partners, etc., all play a role in determining the onset of the quasifission process. However, more experimental evidence is required to confirm the relative importance of all these parameters.

According to Swiatecki [1], there are three milestone configurations that play a very important role in the fusion process: contact configuration, conditional saddle-point configuration, and unconditional saddle-point configuration. If the contact configuration is less elongated than the conditional saddle point, then the system will fuse to form a mononucleus, and if the contact configuration is less elongated than the unconditional saddle-point configuration, then an equilibrated CN will be formed. On the contrary, if the contact configuration is more elongated than the unconditional saddle-point configuration, which can happen at near-barrier energies for deformed reaction partners, the mononucleus will reseparate before complete equilibration, which is the quasifission process. In the present measurements, the different behavior of the mass ratio distributions of the two systems populating the same composite system is indicative of the difference in the dynamical evolution of the two systems over the multidimensional potential energy surface, showing the dependence of entrance channel parameters. In the case of the $^{16}O + ^{194}Pt$ reaction, where $Z_P Z_T$ is 624, the trajectories reach the fully equilibrated CN, after the contact process. The absence of any non-CN behavior in this reaction suggests that the effects of deformation and orientation are not very significant in this case. However, the anomalous behavior of the $^{24}Mg + ^{186}W$ system with $Z_P Z_T$ equal to 888 shows experimental signatures of deviation from CN behavior. It may be conjectured that in this case the trajectories do not completely reach the compact configuration and thus a substantial portion may escape, as a combined effect of elongated contact configuration and subsequent Coulomb repulsion during the dynamical evolution after contact.

IV. SUMMARY AND CONCLUSIONS

Fission fragment mass ratio distributions for the two reactions $^{16}O + ^{194}Pt$ and $^{24}Mg + ^{186}W$, both forming the same CN ^{210}Rn with different entrance channel mass asymmetries, which fall on either side of the critical Businaro-Gallone mass asymmetry value, have been reported. Neither of the reactions studied shows any mass angle correlation. However, the measured mass ratio variance for the $^{24}Mg + ^{186}W$ reaction is much higher than that for the $^{16}O + ^{194}Pt$ reaction at similar excitation energies, implying a deviation from CN behavior at near-barrier energies, although the $Z_P Z_T$ value is much less than 1600. In this case, trajectories are more likely to be deflected away from the compact CN stage, which may be caused by the elongated contact configuration followed by the Coulomb repulsion during the dynamical evolution. But the $^{24}Mg + ^{178}Hf$ reaction [19], which is more symmetric than $^{24}Mg + ^{186}W$, has not shown any signature of the onset of quasifission. It is well known that the onset of quasifission is strongly dependent on the mean fissility χ_m. However, calculations show that the mean fissility for $^{24}Mg + ^{186}W$, $^{30}Si + ^{186}W$, and $^{34}S + ^{186}W$, all reactions that show conclusive evidence of quasifission, are less than 0.723. These experimental results suggest that any dynamical model that attempts to explain the fission fragment mass and angular distributions of fissile and less fissile systems should include $Z_P Z_T$ and the deformations of the collision partners in a systematic way. The apparent observation of larger mass variances for the very asymmetric reaction $^{24}Mg + ^{186}W$ necessitates further investigations with different projectile-target combinations at near-barrier energies.

ACKNOWLEDGMENTS

We are thankful to Pelletron staff, especially R. Joshi and S. Ojha, for providing excellent-quality beams throughout the experiment. We would like to acknowledge the cooperation and encouragement recieved from Dr. B. R. Behera, Dr. Hardev Singh, Dr. J. J. Das, Dr. T. K. Ghosh,

Prof. P. Bhattacharya, Dr. P. D. Shidling, S. Muralithar, and Dr. K. Mahata at various stages of this work. The support received from the target laboratory, especially S. R. Abhilash, the vacuum laboratory, and the data support laboratory is also much appreciated. One of the authors (E.P.) gratefully acknowledges support by a research grant from the University Grants Commission (UGC), New Delhi, for carrying out this work.

[1] W. J. Swiatecki, Phys. Scr. **24**, 113 (1981).
[2] S. Bjornholm and W. J. Swiatecki, Nucl. Phys. A **391**, 471 (1982).
[3] J. P. Blocki, H. Feldmeier, and W. J. Swiatecki, Nucl. Phys. A **459**, 145 (1986).
[4] W. U. Schroder and J. R. Huizenga, in *Damped Nuclear Reactions, Treatise on Heavy-ion Science*, edited by D. A. Bromley (Plenum Press, New York, 1984), Vol. 2, p. 115.
[5] B. B. Back, R. R. Betts, K. Cassidy, B. G. Glagola, J. E. Gindler, L. E. Glendenin, and B. D. Wilkins, Phys. Rev. Lett. **50**, 818 (1983).
[6] M. B. Tsang, H. Utsunomiya, C. K. Gelbke, W. G. Lynch, B. B. Back, S. Saini, P. A. Baisden, and M. A. McMahan, Phys. Lett. B **129**, 18 (1983).
[7] B. B. Back, R. R. Betts, J. E. Gindler, B. D. Wilkins, S. Saini, M. B. Tsang, C. K. Gelbke, W. G. Lynch, M. A. McMahan, and P. A. Baisden, Phys. Rev. C **32**, 195 (1985).
[8] R. Vandenbosch and J. R. Huizenga, *Nuclear Fission* (Academic Press, New York, 1973).
[9] M. Abe, KEK Preprint 86-26, KEK TH-128 (1986).
[10] S. Kailas, Phys. Rep. **284**, 381 (1997).
[11] S. Kailas, K. Mahata, R. G. Thomas, and S. S. Kapoor, Nucl. Phys. A **787**, 259c (2007).
[12] D. J. Hinde, M. Dasgupta, J. R. Leigh, J. P. Lestone, J. C. Mein, C. R. Morton, J. O. Newton, and H. Timmers, Phys. Rev. Lett. **74**, 1295 (1995).
[13] D. J. Hinde, M. Dasgupta, J. R. Leigh, J. C. Mein, C. R. Morton, J. O. Newton, and H. Timmers, Phys. Rev. C **53**, 1290 (1996).
[14] Z. Liu, H. Zhang, J. Xu, Y. Qiao, X. Qian, and C. Lin, Phys. Lett. B **353**, 173 (1995).
[15] J. C. Mein, D. J. Hinde, M. Dasgupta, J. R. Leigh, J. O. Newton, and H. Timmers, Phys. Rev. C **55**, R995 (1997).
[16] A. C. Berriman, D. J. Hinde, M. Dasgupta, C. R. Morton, R. D. Butt, and J. O. Newton, Nature (London) **413**, 144 (2001).
[17] D. J. Hinde, M. Dasgupta, and A. Mukherjee, Phys. Rev. Lett. **89**, 282701 (2002).
[18] R. Bock *et al.*, Nucl. Phys. A **388**, 334 (1982).
[19] R. Rafiei, R. G. Thomas, D. J. Hinde, M. Dasgupta, C. R. Morton, L. R. Gasques, M. L. Brown, and M. D. Rodriguez, Phys. Rev. C **77**, 024606 (2008).
[20] R. G. Thomas, D. J. Hinde, D. Duniec, F. Zenke, M. Dasgupta, M. L. Brown, M. Evers, L. R. Gasques, M. D. Rodriguez, and A. Diaz-Torres, Phys. Rev. C **77**, 034610 (2008).
[21] T. K. Ghosh *et al.*, Phys. Rev. C **79**, 054607 (2009).
[22] R. Tripathi, K. Sudarshan, S. Sodaye, A. V. R. Reddy, K. Mahata, and A. Goswami, Phys. Rev. C **71**, 044616 (2005).
[23] R. Tripathi, K. Sudarshan, S. Sodaye, A. Goswami, and A. V. R. Reddy, Int. J. Mod. Phys. E **17**(2), 419 (2008).
[24] R. Tripathi, K. Sudarshan, S. K. Sharma, K. Ramachandran, A. V. R. Reddy, P. K. Pujari, and A. Goswami, Phys. Rev. C **79**, 064607 (2009).
[25] S. Appannababu *et al.*, Phys. Rev. C **80**, 024603 (2009).
[26] T. K. Ghosh *et al.*, Nucl. Instrum. Methods Phys. Res. A **540**, 285 (2005).
[27] A. Jhingan, P. Sugathan, K. S. Golda, R. P. Singh, T. Varughese, H. Singh, B. R. Behera, and S. K. Mandal, Rev. Sci. Instrum. **80**, 123502 (2009).
[28] R. K. Choudhury *et al.*, Phys. Rev. C **60**, 054609 (1999).
[29] V. E. Viola, K. Kwiatkowski, and M. Walker, Phys. Rev. C **31**, 1550 (1985).
[30] A. J. Sierk, Phys. Rev. C **33**, 2039 (1986).
[31] V. S. Ramamurthy and S. S. Kapoor, Phys. Rev. Lett. **54**, 178 (1985).
[32] C. Lebrun, F. Hanappe, J. F. LeColley, F. Lefebvres, C. Ngo, J. Peter, and B. Tamain, Nucl. Phys. A **321**, 207 (1979).
[33] M. G. Itkis and A. Ya. Rusanov, Phys. Part. Nucl. **29**, 160 (1998).
[34] G. D. Adeev, I. I. Gontchar, V. V. Pashkevich, N. I. Pischasov, and O. I. Serdyuk, Phys. Part. Nucl. **19**, 1229 (1988).
[35] E. G. Ryabov, A. V. Karpov, and G. D. Adeev, Nucl. Phys. A **765**, 39 (2006).
[36] K. Hagino, N. Rowley, and A. J. Kruppa, Comput. Phys. Commun. **123**, 143 (1999).
[37] D. J. Hinde, R. J. Charity, G. S. Foote, J. R. Leigh, J. O. Newton, S. Ogaza, and A. Chattejee, Nucl. Phys. A **452**, 550 (1986).
[38] K.-T. Brinkmann, A. L. Caraley, B. J. Fineman, N. Gan, J. Velkovska, and R. L. McGrath, Phys. Rev. C **50**, 309 (1994).
[39] G. N. Knyazheva *et al.*, Phys. Rev. C **75**, 064602 (2007).
[40] A. Gavron, Phys. Rev. C **21**, 230 (1980).
[41] A. Saxena, A. Chatterjee, R. K. Choudhury, S. S. Kapoor, and D. M. Nadkarni, Phys. Rev. C **49**, 932 (1994).
[42] S. Raman *et al.*, At. Data Nucl. Data Tables **78**, 1 (2001).